

Dielectric Investigation of the Low-Temperature Water Dynamics in the Poly(vinyl methyl ether)/H₂O System

S. Cerveny,^{*,§} J. Colmenero,^{†,§} and A. Alegría^{†,‡}

Unidad de Física de Materiales, Centro Mixto CSIC-UPV/EHU, and Departamento de Física de Materiales, Universidad del País Vasco (UPV/EHU), Facultad de Química, Apartado 1072, 20018, San Sebastián, Spain, and Donostia Internacional Physics Center, Paseo Manuel de Lardizabal 4, 20018, San Sebastián, Spain

Received April 18, 2005; Revised Manuscript Received June 6, 2005

ABSTRACT: Broadband dielectric spectroscopy (10^{-1} – 10^6 Hz) and differential scanning calorimetry measurements have been performed to study the molecular dynamics of water solutions of poly(vinyl methyl ether) (PVME) in the concentration region up to 50 wt % and in the temperature range from 150 to 250 K in order to investigate the low-temperature water dynamics in this system. A symmetric spectrum due to reorientation of water molecules inside the rigid polymer matrix was observed for all hydration levels. However, the dielectric relaxation results evidence that different “water types” can be distinguished depending on the hydration level. For moderate water content (ca. below 30 wt %) the water molecules have both orientational and translational restrictions. For high water contents the excess water is able to fully reorientate at low temperatures and to crystallize above 230 K. Furthermore, our dielectric results support the idea that water molecules are not uniformly distributed among the monomeric units of PVME.

Introduction

Water is unquestionably one of the most studied compounds in both physics and chemistry. Because of the fact that each water molecule can interact with four neighbors, hydrogen bonding allows the creation of an extended network of molecules. In liquid water the connectivity of this network is subject to continuous fluctuations in local structure and molecular reconfigurations that break and form individual hydrogen bonds. Because of the fact that bulk water crystallizes on cooling, the study of water solutions (with sugars, alcohols, proteins, etc.) or in confined geometries has been widely investigated by various experimental methods such as nuclear magnetic resonance (NMR),¹ dielectric relaxation,² Raman spectroscopy,^{3,4} differential scanning calorimetry (DSC),^{4,5} simulations,⁶ and neutron scattering.⁷ The purpose of such studies has been centered on the structure of water in a supercooled state. In particular, water in polymers is one of the topics widely studied but the majority of these works focused on the effects on bulk properties of the host material instead of water dynamics in the polymer matrix. A lot of effort has been made in understanding water dynamics in biological systems such as proteins. However, it is worth noticing that these systems are extremely complex since movements of the host materials directly affect the water dynamics. Contrarily, synthetic polymers offer the possibility to study the water dynamics in a better controlled environment because the polymeric chains often remain frozen in the temperature range where the water dynamics is relevant.

In the opinion of most of the researchers in the polymer community water in polymers, at temperatures below the freezing point, can be categorized^{8–10} into

three types: “free water”, which is qualitatively similar to bulk water with respect to translational and rotational movements and freezes at the usual freezing temperature; “intermediate water” or “loosely bound water”, which is translational restricted but retains at least some rotational movements and freezes at temperatures lower than the usual freezing points; and “nonrotational bound water” or “unfrozen bound water”, which cannot freeze at the usual freezing point and is basically totally bound to the polymer via more than one hydrogen bond. It is important to note that in some water–polymer systems (poly(vinyl alcohol), poly(*N*-vinylpyrrolidone), and poly(vinyl methyl ether)) water crystallization is inhibited at high polymer concentration, likely because water molecules are strongly bound to the polymer matrix. For the last two polymers the formation of a complex between the polymer and water molecules has been proposed in the literature.^{9–11} Nevertheless, there is not a clear explanation of the molecular mechanisms of such complex formation.

It is well-known that poly(vinyl methyl ether), PVME, is a water-soluble polymer which has the lower critical solution temperature with water at around 35 °C.¹² The intermolecular interactions between PVME and water are supposed to be the responsible of its bimodal phase diagram, and for this reason it is useful to have a well understanding of its hydration behavior. At the molecular level, PVME has hydrophilic sites (ether oxygen) that can be hydrogen bonded with the neighboring water molecules and hydrophobic sites (mainly methyl groups) that can disrupt the water structure around the polymer chains. Aqueous solution of PVME has been studied by different techniques as near-infrared,¹³ calorimetric,¹⁴ dielectric spectroscopy,¹⁵ and NMR.¹⁶ Mainly from the fact that crystallization of water is inhibited at water concentration (c_w) lower than 39 wt %, it was supposed that PVME makes a complex with water ($c_w \approx 39$ wt %, means ≈ 2.06 water molecules per monomeric unit of PVME). The submerged presumption for the complex formation is that all the water molecules

[†] Unidad de Física de Materiales, Centro Mixto CSIC-UPV/EHU.

[‡] Universidad del País Vasco (UPV/EHU).

[§] Donostia Internacional Physics Center.

are equally distributed among each monomeric unit. However, there is not agreement on how many molecules form this complex. Additionally and contradictory with these results, a recent study in the literature¹⁷ using simulation of infrared spectral bands shows that water on PVME is not equally distributed even if the hydrated polymer is in the homogeneous phase. In addition, recent small-angle neutron scattering results in deuterated samples¹⁸ do not support the existence of a stable molecular complex even at high concentration of PVME, although the measurements were made at temperatures around 300 K where the complex formation could not be clearly seen.

In this work we have investigated the properties of PVME/H₂O mixtures by both dielectric and calorimetric methods. Our experiments have been focused on the water dynamics in the low-temperature range (150–200 K) where the PVME matrix remains essentially immobile since the glass transition temperature (T_g) of dry PVME is around $T_g \approx 250$ K. In particular, dielectric relaxation spectroscopy is suited for the investigation of the H-bond rearrangement dynamics due to its ability to monitor the motion of water dipole. There are two remarkable reasons to study the water dynamics using a polymer as a host material: (i) the presence of the polymer acts as inhibitor of crystallization and (ii) because the dielectric signal from the glassy polymer is negligible as compared to that of the water molecules.

Experimental Section

PVME, $-(\text{CH}_2-\text{CH}(\text{OCH}_3))_n-$, in aqueous solution (50 wt %) was purchased from Aldrich Chemical and was used without any further purification. The estimated weight-average molecular weight (M_w) and polydispersivity of this polymer are 21.9 kg/mol and 3, respectively.

Different hydration values were obtained by evaporating water from the 50 wt % sample under normal room conditions. The evaporation was carried out directly on the electrodes used for dielectric relaxation measurements. Final water content was determined by weighing the samples. Samples with a water concentration (c_w) of 50, 45, 40, 35, 30, 20, 10, and 2 wt % were obtained in this way. It should be noted that these values were based on the overall water polymer mixture. A small part of hydrated samples were then quickly crimp-sealed into the DSC pans for calorimetric measurements. Water loss or uptake was found to be negligible during this process. Each sample was measured immediately after reaching the desired water content.

A broadband dielectric spectrometer, Novocontrol Alpha analyzer, was used to measure the complex dielectric function, $\epsilon^*(\omega) = \epsilon'(\omega) - i\epsilon''(\omega)$, $\omega = 2\pi f$, in the frequency (f) range from $f = 10^{-1}$ Hz to $f = 10^6$ Hz. The samples were placed between parallel gold-plated electrodes with a diameter of 30 mm and were typically 0.1 mm thick. After cooling at a rate of 10 K/min, isothermal frequency scans recording $\epsilon^*(\omega)$ were performed every 10 deg over the temperature range 130–290 K. The sample temperature was controlled with stability better than ± 0.15 K.

A DSC Q1000 TA Instrument was used in standard and temperature-modulated (TMDSC) modes. Standard DSC measurements were performed using cooling and heating rates of 10 K/min. TMDSC experiments were carried out on heating with a temperature amplitude $T_a = 0.8$ K, a modulation period of $t_p = 60$ s ($\omega = 0.105$ rad s⁻¹), and 5 K/min of underlying heating rate. Hermetic aluminum pans were used for all the materials, and the helium flow rate used was 25 mL/min. The sample weights were about 20 mg.

Results

A. Calorimetric Results. The differential scanning calorimetry measurements were used not only to detect

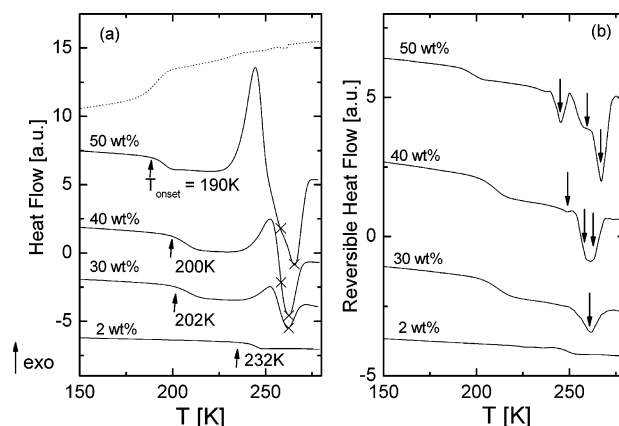


Figure 1. (a) TMDSC scans of PVME at different water concentration, during heating at a rate of 5 K min⁻¹. The dotted line shows a cooling scan at a rate of 10 K min⁻¹ for a sample with $c_w = 50$ wt %. T_{onset} indicates the onset of the glass transition. (b) Reversible part of the heat flow. The arrows in the graph show different melting points for the bound water presented in the samples.

the glass transition temperatures (T_g) of the solutions but also to detect possible crystallization on cooling as well as cold-crystallization and melting on heating.

DSC scans, showing the heat flow for some representative water contents of PVME–aqueous solutions during heating, are given in Figure 1a. These scans are for samples studied immediately after preparation. Additionally, a cooling scan for the sample with the higher water content ($c_w = 50$ wt %) is shown in the same figure. This curve reflects the fact that using this cooling rate no crystallization on cooling occurs in the samples for any water content. Thus, cooling at 10 K/min, an amorphous material is obtained at low temperatures.

Heating scans in Figure 1a show the three typical regions for PVME–water solutions: a glass transition followed by a cold crystallization¹⁹ and the subsequently melting. Cold crystallization is observed for water concentrations between 50 and 30 wt %, while it is absent for lower water contents. Thus, the water present in concentrations below 30 wt % is assumed to be more efficiently bound to the polymer chain than that in the samples with higher water content.

Two endotherms of water melting are observed in Figure 1a for high water contents (> 30 wt %) while only one is observed for 30 wt %. Because of the superposition between cold crystallization and melting, the endotherms are not clearly seen. To resolve this overlapping, measurements were made in modulated mode because in this way it is possible to isolate reversible phenomenon. An inspection of the reversible heat flow in Figure 1b shows different melting points for the samples during the hydration process. Obviously all the melting temperatures observed are lower than 273 K. This depression in temperature has been commonly attributed to some interaction of the water with the host polymer chain.²⁰

Glass transition temperatures for the PVME–water system depend on the concentration as shown in Figure 2a, in agreement with reported data.¹⁴ It is easy to see that T_g values do not vary in a smooth way with the water concentration. Instead, the T_g dependence on water concentration shows a sudden change at around 30 wt %. For concentrations lower and higher than 30 wt %, T_g decreases monotonically with increasing water

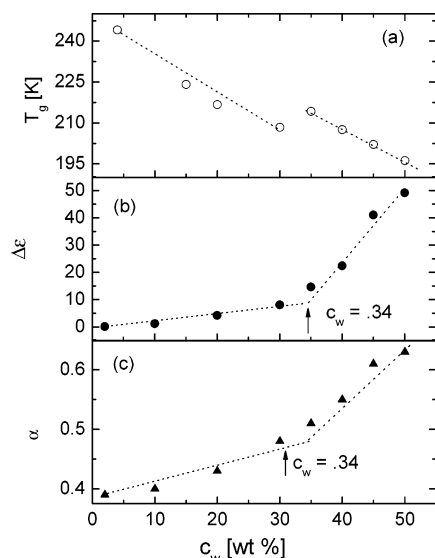


Figure 2. Variation of T_g (a), $\Delta\epsilon$ (b), and α (c) with water content. $\Delta\epsilon$ and α are the averaged values taken from Figure 5. Critical water concentration, $c_c = 34$ wt %, in (b) and (c) was calculated as the intersection of the two dotted lines.

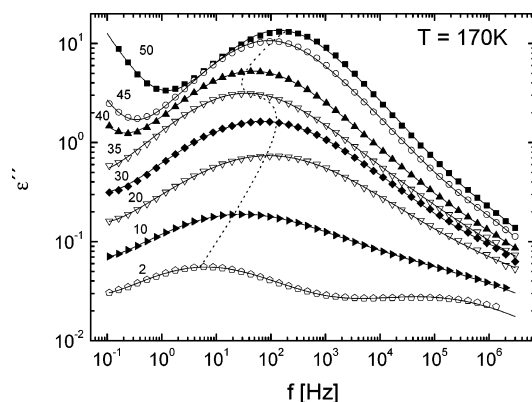


Figure 3. Loss component, ϵ'' , of the complex dielectric permittivity, $\epsilon^*(f)$, of PVME–water systems at a fixed temperature. The number in each curve represents the water content in the sample. The dotted line indicates the nonmonotonic behavior of the maximum of the peak when increasing water content.

content, as expected for homogeneous solutions. This change in the behavior of T_g with the water content is an additional indication that the water structure changes rather suddenly at concentrations about 30 wt %.

B. Dielectric Results. It is important to note that all the dielectric results in this work are comparable with those obtained by DSC as we used the same cooling procedure for both measurements.

Isothermal data of the loss peak ϵ'' for PVME aqueous solution at $T = 170$ K are shown in Figure 3. A very broad peak is observed for all the concentrations. Additionally, a weak relaxation is seen in the high-frequency range for low water concentration. This relaxation is in good agreement with the secondary relaxation of dry PVME reported elsewhere.²¹ The frequency, f_{\max} , calculated from the frequency at the maximum of ϵ'' peak does not present a monotonic behavior with the water content as shown in Figure 3 (dotted line). f_{\max} increases with increasing water contents up to 30 wt %; however, the frequency peak shift back slightly to lower frequencies at $c_w = 35$ wt

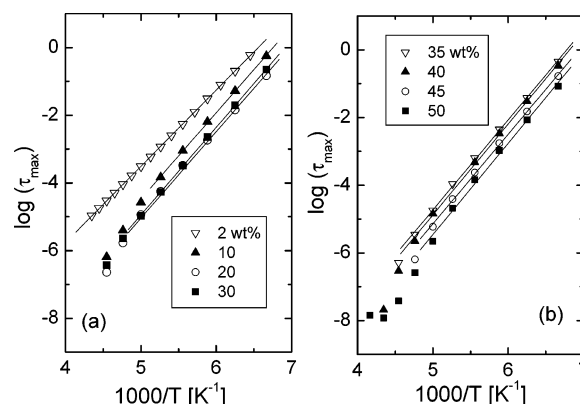


Figure 4. (a, b) Plot of the characteristic relaxation times, τ_{\max} , for PVME aqueous solutions. The results of fitting Arrhenius functions to the data are shown with solid lines. At temperatures higher than the calorimetric T_g , the relaxations times speed up from the Arrhenius behavior.

Table 1. Activation Energy (E) and Preexponential Factor ($\log(\tau_0)$) Obtained from the Arrhenius Equation Applied to the Line in Figures 4a,b for All the Concentrations^a

c_w [wt %]	$\log(\tau_0)$	E [eV]
2	-14.3 ± 0.1	0.45 ± 0.01
10	-17.5 ± 0.4	0.51 ± 0.03
20	-17.1 ± 0.2	0.49 ± 0.01
30	-17.9 ± 0.1	0.51 ± 0.01
35	-17.8 ± 0.1	0.52 ± 0.01
40	-17.9 ± 0.2	0.52 ± 0.01
45	-18.0 ± 0.1	0.51 ± 0.01
50	-18.1 ± 0.3	0.51 ± 0.01
excess water, $c_w = 35$ wt %	-17.1 ± 0.1	0.51 ± 0.01
excess water, $c_w = 50$ wt %	-18.0 ± 0.3	0.50 ± 0.01

^a In the last two rows the parameters of the Arrhenius equation for the excess water contribution for the samples with $c_w = 35$ and 50 wt %, respectively.

%. At this concentration, the monotonic behavior is recovered.

In Figure 4a,b we show the temperature dependence of the relaxation times, $\tau_{\max} = 1/(2\pi f_{\max})$. Note that defined in this way the relaxation times were obtained independently of any fitting frames. The relaxation times τ_{\max} for PVME aqueous solutions show an Arrhenius-like behavior for temperatures lower than 200 K. Above this temperature, there is a systematic reduction of the relaxation time with respect to the extrapolation of the line, and this effect is more pronounced when increasing water content. The corresponding temperature range is in good agreement with the onset of the glass transition for each solution as measured by DSC (see Figure 1b), thus indicating that movements of the polymer host material affect this relaxation. For this reason, we will analyze this relaxation for temperatures up to 200 K. In this range the relaxation times were fitted by an Arrhenius temperature dependence: $\tau(T) = \tau_0 \exp(E/kT)$, where for a simple activated process τ_0 would correspond to a molecular vibration time and E would be the activation energy. The fitted values for E and τ_0 are shown in Table 1. While the activation energy was roughly independent of the water concentration, unphysical low values of τ_0 were obtained. This point will be discussed below.

Since most dielectric data are collected in the frequency domain, semiempirical frequency-dependent

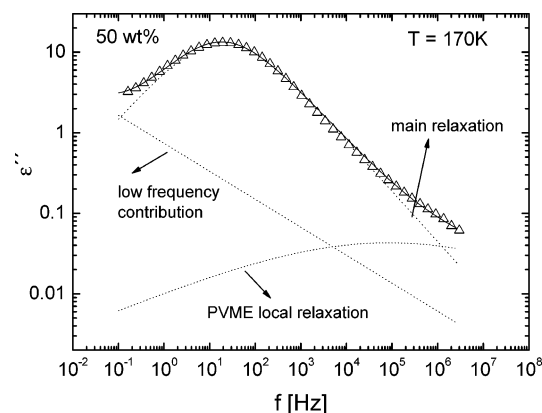


Figure 5. Dielectric loss $\epsilon''(f)$ vs frequency for $c_w = 50$ wt %. The solid line through the data points is a least-squares fits to a superposition of a power law (dashed line) and the imaginary part of two Cole–Cole functions. Each Cole–Cole is also shown separately.

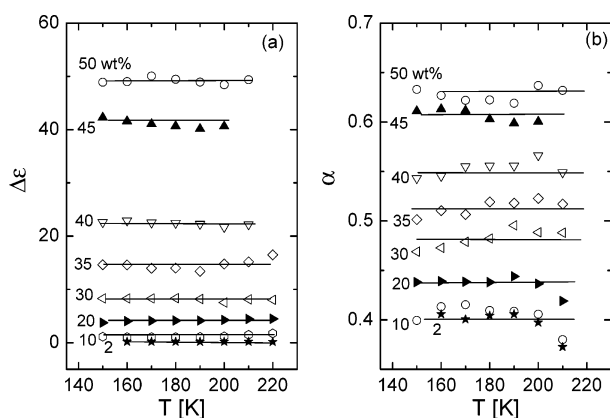


Figure 6. (a, b) Dielectric strength ($\Delta\epsilon$) and shape parameter (α) vs temperature for the observed process for all water contents. The solid lines through the data represent the average value for each water content.

functions are often used to describe the data. The most common is the Havriliak–Negami (HN) expression²¹

$$\epsilon^*(\omega) = \epsilon_\infty + \frac{\epsilon_s - \epsilon_\infty}{[1 + (i\omega\tau_{\text{HN}})^\alpha]^\gamma} \quad (1)$$

where ϵ_∞ and ϵ_s are the unrelaxed and relaxed values of the dielectric constant, τ_{HN} is a relaxation time, and ω is the angular frequency. In eq 1 α and γ are shape parameters ($0 < \alpha, \alpha\gamma \leq 1$). Setting $\gamma = 1$, a symmetrical function is obtained (Cole–Cole function²³) which is widely used to describe secondary relaxations in glassy materials. An asymmetric Cole–Davidson (CD) function²⁴ is obtained with $\alpha = 1$.

An example of the fitting procedure is represented in Figure 5. A symmetrical Cole–Cole (CC) function was used to fit the main relaxation. Additionally, a second CC was added at high frequencies to account possible weak effects associated with the local motions of PVME.²¹ A small contribution is also seen at low frequencies, and to account for that, a power law term was added.

The relaxation strength ($\Delta\epsilon = \epsilon_s - \epsilon_\infty$) and the shape parameter (α) of the main process as obtained from the fits are shown in parts a and b of Figure 6, respectively. Clearly, $\Delta\epsilon$ and α are almost temperature independent, but both are greatly affected by the amount of water. The full lines in Figure 6 represent an average value of $\Delta\epsilon$ and α for each sample in the whole temperature

range considered. Changes in these values were plotted as a function of water content in Figure 2b,c. It is immediately clear that both $\Delta\epsilon$ and α increase linearly with the concentration until around 30 wt %. After that concentration, a stronger increase of both parameters is observed. It is remarkable that at $c_w = 30$ wt % there are, on average, almost 1.5 water molecules per monomer of PVME. It is also noteworthy that the formation of a stable molecular water–polymer complex was proposed in the literature¹¹ for concentrations around 35 wt %. The strong increase in the relaxation strength for concentration higher than 30 wt % cannot come only from the increasing number of relaxing units. Instead, it indicates an increase in the water mobility. Once more, a water concentration of about 30 wt % in the samples is the limit for two different behaviors in its dynamic.

Note that the large broadening of the relaxation peak in the course of dehydration of the sample (about 3 frequency decades at half-maximum as compared to 1.14 decades for a single Debye process) also indicates a broad distribution of the relaxation times, suggesting a rather inhomogeneous water molecule environment.

Summarizing, water dynamics looks different depending on the hydration level, and simultaneously an inhomogeneous water molecule environment is observed from the dielectric data for each mixture. From this we follow that a “complex-like” is formed at the investigated low temperatures and compositions, in the sense that we cannot ensure that the water molecules more strongly bounded to the PVME chain remain so permanently.

Discussion

We will first consider the molecular origin of the relaxation spectrum shown in Figure 3. In the temperature range analyzed (150–200 K) there is basically no contribution of PVME to the dielectric spectra because both the weak contribution of its local movements (the strength of the secondary relaxation of pure PVME is 1 order of magnitude lower than that measured for the solutions, at least for water contents higher than 10 wt %) and the arrest of the polymer segmental dynamics. Then, it is expected that the observed spectrum reflects the water mobility in the PVME water mixtures. To confirm this hypothesis, deuterium isotopic substitution was used in one of the samples ($c_w = 50$ wt %). It is commonly assumed that the interactions (hydrogen or deuterium bonds) are not significantly modified by the isotopic substitution. However, because of the higher mass of deuterium compared to hydrogen, the relaxation times usually results slower than those in the nondeuterated hydrogen bond networks.^{25,26} Figure 7 shows the relaxation times for both deuterated and protonated samples. As expected, the relaxation times are similar for both isotopic forms but slightly faster for protonated samples whereas $\Delta\epsilon$ and α in the fitting (Figure 7, insets a and b) are very close to the protonated one (the fitting procedure was the same as in the case of the protonated samples). Therefore, this is a strong indication that the relaxation spectrum in Figure 3 reflects mainly the water mobility in the PVME mixtures.

All the dielectric properties, the shape of the spectrum, the relaxation times, and $\Delta\epsilon$ simultaneously change at a concentration around $c_w = 30\%$ where a change in T_g is found. By extrapolating the two lines in Figure 2b, they intersect at a critical water concentra-

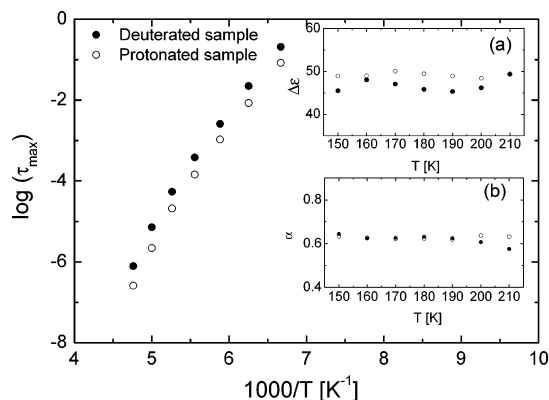


Figure 7. Comparison between the relaxation times (τ_{\max}) for deuterated and protonated samples with a concentration of 50 wt %. (a) Dielectric strengths ($\Delta\epsilon$) and (b) shape parameter (α) vs temperature. Open symbols denote the protonated samples and filled symbols the deuterated samples.

tion, $c_c = 34$ wt %, where the evolution of the dielectric properties with c_w changes. As aforementioned, this concentration range corresponds to that where the formation of a molecular complex between water and PVME has been suggested in the literature.^{11,13–15} Depending on the source and the experimental method used to investigate such complex formation, the number of water molecules per monomer of PVME is estimated to be close to 2. From our dielectric results, an average of 1.7 water molecules per monomeric unit would produce a complex-like structure between water and PVME at least in the low-temperature range (150–200 K).

To validate the idea of a complex-like formation, we prepared a new sample which was cooled using a slow rate (1 K/min). This slow cooling rate would allow some water to crystallize during cooling. In particular, at $c_w = 50$ wt % significant crystallization takes place on cooling, producing a separation into ice and a solution which differs from the previous one in concentration.¹⁴ The dielectric measurements on this partially crystallized sample reveal new information about its behavior. Figure 8 shows the loss component of the complex permittivity (ϵ''), relaxation times, and relaxation strength for this sample. It is easy to see a bimodal loss peak in the dielectric response. While the slower peak could be attributed to the presence of ice formed during cooling, the faster one corresponds well, in time scale and intensity (see insets a and b in Figure 8), with that measured for the sample with 30 wt %. From this, we follow that after crystallization the sample with 50 wt % shows a dielectric response with a component similar to the sample with 30 wt % and another slower component which would be related to the presence of some water molecules in an ice matrix or most likely with interfacial polarization effects associated with the presence of the ice phase. No further attempts were made to clarify the molecular origin of that slow component.

Therefore, our dielectric results support the existence of complex-like formation at low temperatures between water and PVME in which the water molecules concentration could be as high as 34 wt %. Taking into account the complex-like formation at low temperatures, three different scenarios could be outlined for water dynamics in PVME, depending on water content.

Very Low Water Content ($c \approx 2$ wt %). At this water content, there is around 1 water molecule each 15 PVME monomeric units. The water molecule is likely

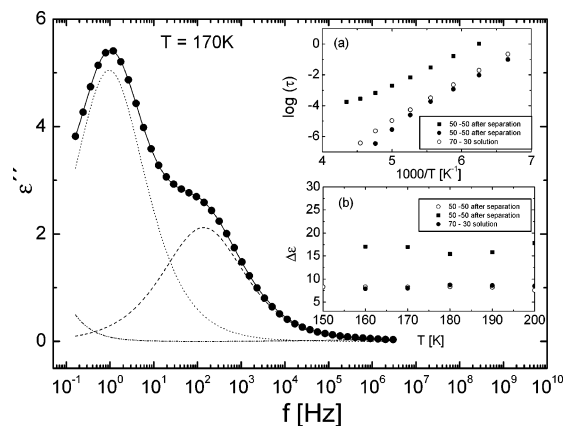


Figure 8. Dielectric loss for a partially crystallized sample with an initial water concentration of 50 wt %. Two peaks in ϵ'' are clearly seen. The solid line through the data points is a least-squares fits to a superposition of the imaginary part of two Cole–Cole functions and a power law (dashed line). Inset (a): relaxation times the values of the sample the partially crystallized sample with an original water concentration of 50 wt %. The values of the sample with 30 wt % are included for comparison. Inset (b): relaxation strength for the same samples as in inset (a).

almost isolated from the other water molecules in the system, and it is bounded to the polymer likely via the ether oxygen in PVME, since they are the most hydrophilic sites in the PVME matrix. Then, individual reorientations of the water molecule will be more or less hindered. The relaxation strength is very low because a few water molecules are involved in this relaxation, and the reorientations are rather restricted. The multiplicities of environments seen for the roughly isolated water molecule introduce a distribution of the relaxation times around the most probable value τ_{\max} . Consequently, there is a broad relaxation (α parameter is rather low). This behavior (in the regime of low hydration) was also observed for water molecules in other polymers and biological materials and was attributed to a local β -like water process.²⁷ Finally, it is important to note from Table 1 that the value of τ_0 obtained from the Arrhenius plot was $10^{-14.4}$ s, which is not far from the reciprocal of typical vibrational frequencies, and therefore the observed relaxation would essentially reflect thermally activated molecular motions, with small activation entropies according with the Starkweather approach.^{28,29} Under this approximation, this relaxation does not show significant cooperative effects and can be associated with the local movements of individual water molecules bounded to the polymer matrix. The activation energy determined (~ 0.45 eV) would be therefore a measure of the average barrier height separating two equivalent energy minima.

Intermediate Water Content ($10 \leq c_w < 34$ wt %). For water content (c_w) between 10 and 30 wt % (this means between 0.36 and 1.5 molecules of water per PVME monomer in average), it is expected that the water molecules are closer to each other as water content increases. Thus, the environment around a water molecule will become more uniform. As a result, the width of the dielectric response will decrease (α parameter gets higher). The relaxation strength also increases because more relaxing units are involved in the relaxation although the orientation restrictions remain because water molecules are robustly linked to the PVME matrix, giving rise to the complex-like

structure which would make unfavorable water crystallization. In this region T_g values (see Figure 2a) decrease with increasing water content as expected for homogeneous solutions. Turning to the relaxations times, we found that they have an Arrhenius temperature dependence (values for E and $\log(\tau_0)$ are reported in Table 1). The fact that the distribution width does not change much with temperature indicates that the origin of such a distribution is hardly associated with significant differences among the energy barriers but more likely to different values of the preexponential factor in the Arrhenius equation. Furthermore, the unphysical low values of τ_0 obtained suggest that the local water relaxations do not fit Starkweather's definition^{28,29} of a simple relaxation, showing cooperative effects. Since these effects are already noticeable for $c_w = 0.10$ wt % (and average of 0.36 water molecules per PVME monomer), it seems that the water molecules do not distribute uniformly, but more likely they would go first to the more favorable sites. This would give rise to some kind of aggregate where the water molecules would move together. In this picture, the difference in cooperativity (number of water molecules belonging to the aggregates) would be the main reason for the broadly distributed values of τ_0 .

High Water Content ($34 < c_w \leq 50$ wt %). At this hydration level, there are from ~ 1.7 to ~ 3.3 water molecules per PVME monomer in average. The complex-like structure between water molecules and PVME has already been formed, and the excess water molecules cannot be linked directly to polymer chain sites but they will form a second hydration shell. Therefore, water–water interactions would dominate the dynamics of this excess water. As a result, the excess water molecules, not in direct contact with the polymer, would behave much like bulk water. These water molecules could orientate more easily than before because water is interacting with other water molecules instead interacting directly with the polymer. For this reason, the relaxation strength grows more than expected according to the extrapolation from lower concentrations as shown in Figure 2b. Additionally, the spectra become narrower than for lower water contents because the environment seen by the new water molecules would become more and more homogeneous. In addition, the new water molecules in this regime would have no much translational restrictions, and they are able to crystallize on cooling at low rates. The relaxation times are monotonically faster with the addition of water, indicating that the excess water is more mobile likely because they would be less efficiently bounded to the hydrophobic sites. As in the precedent case, unphysical values of τ_0 were obtained, indicating a high cooperativity, which is consistent with the fact that, at this stage, water molecules are surrounded by (and move with) other water molecules.

Summarizing, there are three different categories of water in the hydration process of PVME water mixtures. The first one represents the isolated molecule (no significant cooperativity) and the second one the water strongly bound to the PVME which participates in the complex-like formation (unphysical τ_0 indicating significant cooperativity). In these two situations the reorientation is markedly restricted and the translational motions are nearly avoided. The last category of water represents the water in excess to the complex-like structure which is essentially surrounded by (and

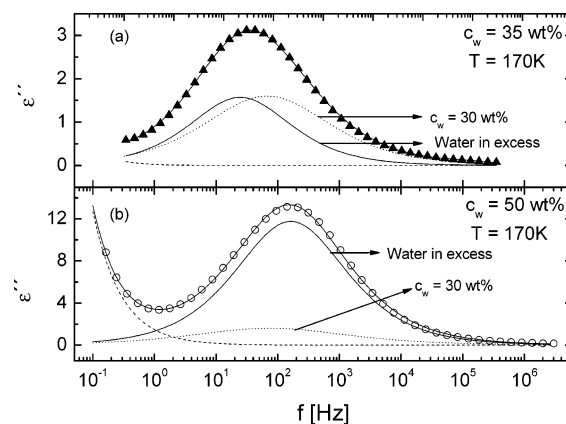


Figure 9. Dielectric loss vs frequency for a water concentration of 35 wt % (a) and 50 wt % (b). The solid line through the data points represents the least-squares fits to a superposition of a power law (dashed line), the imaginary part of a Cole–Cole function in dotted line (for water linked to PVME with the same relaxation time and shape parameters as for the sample with 30 wt %), and another Cole–Cole function to take into account the water in excess (full line) (see text).

moves with) other water molecules showing also a significant cooperativity (unphysical low τ_0). Each of these water categories has their own characteristics in the dielectric spectra as we will show in the next paragraph.

On the basis of the discussion above, two samples ($c_w = 35$ and 50 wt %) were considered in order to account for the dynamics of water molecules in PVME polymer solutions. For each sample we used a superposition of two functions representing the two different behaviors at high water content. Additionally, it is also possible to consider the response of isolated water, but since the relaxation strength is very low because the probability of such a situation decreases drastically when increasing water content, we do not consider this relaxation in the following analysis. To describe the data at each temperature, we used a Cole–Cole equation for the processes related with the water molecules H-bonded to PVME (modeled with the same relaxation spectrum as that measure for the sample with $c_w = 30$ wt %). For the remaining of the dielectric signal we used another Cole–Cole function to take into account the behavior of the excess of water. In the fitting procedure only the parameters corresponding to the second Cole–Cole function were free. In Figure 9 it is possible to see how these two processes, each one related to different states of water in the samples, allow a good description of the experimental dielectric relaxation. Figure 10 shows the results of this fitting procedure: relaxation times, relaxation strength, and width of the relaxation of the excess water as a function of the temperature. The parameters corresponding to the Arrhenius equation fitting the relaxation times are depicted in Table 1. Thus, the dielectric spectra at high water concentration in PVME aqueous solutions can be considered as arising from two different water contributions.

Combining results of dielectric spectroscopy with those of computer simulations, the time scales of the cooperative relaxation process of H-bond liquids (water, alcohols, or their mixtures) are generally shown as the probability that molecules in the system find a new H-bond partner.^{30–32} The fact that the values of activation energy shown in Table 1 do not vary much with the hydration level also agrees with this idea. It also

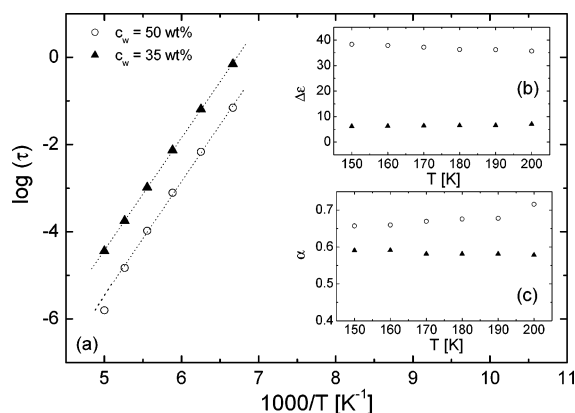


Figure 10. Relaxation times vs $1000/T$ for excess water in two samples (35 and 50 wt %). Insets (b) and (c): dielectric strength and shape parameters for water in excess for the same samples shown in (a).

provides a consistent explanation of the decrease of the relaxation times and the cooperative effects observed. At low water contents, the water molecules have difficulty finding a partner, and then the dipole orientation cannot occur efficiently. Increasing water content the probability of locating a partner to be H-bonded increases (water molecules are surrounded by other water molecules), and this produces simultaneously the reduction of the relaxation times and significant cooperativity. This tendency continues until water molecules in excess with respect to the complex-like structure appear. In the first stages the excess water molecules would again find difficultly moving cooperatively with another water molecule of the same type, and therefore the relaxation rate of these molecules would be small. As a consequence of the relatively high contribution to the dielectric relaxation of this excess water, the overall relaxation process is first slowed down and as more water is added again speeds up monotonically.

Conclusions

The results obtained by dielectric spectroscopy and differential scanning calorimetric on PVME aqueous solutions with water content up to 50% evidence that at low temperatures two different types of water molecules exist in the solutions with water content above 34%. In the lower water concentration range our results indicate that water molecules interact strongly with the polymer matrix, which suppresses the translational motions of the water molecules and limits their reorientation. This manifests respectively as an increasing difficulty for water to crystallize and a dielectric relaxation weaker than that expected from water molecules without orientational restrictions. In the high water concentration range these molecules coexist with the new water molecules that are not able to interact directly with the polymer (all the hydrophobic sites in the polymer would be occupied) but are H-bonded to the existing water molecules. This excess water behaves more like bulk water since it tends to crystallize easily and has a stronger contribution to the dielectric relaxation indicative of the losing of the reorientation restrictions. However, the low-temperature dynamics of both types of water molecules show some common features. In both cases, the temperature dependence of the relaxation times follows nicely an Arrhenius behavior, being the corresponding activation energies rather similar. On the other hand, the prefactor of the Arrhe-

nus equation is much smaller than that expected from the reciprocal of a typical phonon frequency. These results suggest that the water molecules are not moving independently of each other, but on the contrary they would form some kind of aggregate where the water molecules move together. Nevertheless, although the dynamics of both types of water molecules show significant heterogeneity, this is much less pronounced for the water molecules that are not directly bounded with the polymer. It should be emphasized that this picture would apply at low temperatures where the polymer matrix is essentially immobile but not necessary at higher temperatures because both the motion of the polymer segments and the increase of the thermal energy could produce the interchange of the water molecules which would make the differences in behavior between the two types of water molecules disappear.

Acknowledgment. The authors acknowledge the support of the University of Basque Country and the Basque Government Project UPV/EHU, 206.215-G20/98, and the Spanish Ministry of Education Project MAT2004-01017.

References and Notes

- (1) McCormick, M.; Smith, R. N.; Graf, R.; Barrett, C. J.; Reven, L.; Spiess, H. W. *Macromolecules* **2003**, *36*, 3616–3625.
- (2) Mijovic, J.; Zhang, H. *Macromolecules* **2003**, *36*, 1279–1288.
- (3) Marinov, V. S.; Nickolov, Z. S.; Matsuura, H. *J. Phys. Chem. B* **2001**, *105*, 9953–9959.
- (4) McBrierty, V. J.; Martin, S. J.; Karasz, F. E. *J. Mol. Liq.* **1999**, *80*, 179–205.
- (5) Faivre, C.; Bellet, D.; Dolino, G. *Eur. Phys. J. B* **1999**, *7*, 19–36.
- (6) Goudeau, S.; Charlot, M.; Muller-Plathe, F. *J. Phys. Chem. B* **2004**, *108*, 18779–18788.
- (7) Swenson, J.; Bergman, R.; Howells, W. S. *J. Chem. Phys.* **2000**, *113*, 2873–2879.
- (8) Quinn, F. X.; Kampff, E.; Smyth, G.; McBrierty, V. J. *Macromolecules* **1988**, *21*, 3191–3198.
- (9) Higuchi, A.; Komiya, J.; Iijima, T. *Polym. Bull. (Berlin)* **1984**, *11*, 203–208.
- (10) de Dood, M. J. A.; Kalkman, J.; Strohhofer, C.; Michielsen, J.; van der Elksen, J. *J. Phys. Chem. B* **2003**, *107*, 5906–5913.
- (11) Meeussen, F.; Bauwens, Y.; Moerkerke, R.; Nies, E.; Berghmans, H. *Polymer* **2000**, *41*, 3737–3743.
- (12) Schafer-Soenen, H.; Moerkerke, R.; Berghmans, H.; Koningsveld, R.; Dusek, K.; Solc, K. *Macromolecules* **1997**, *30*, 410–416.
- (13) Maeda, H. *J. Polym. Sci., Part B: Polym. Phys.* **1994**, *32*, 91.
- (14) Zhang, J. M.; Berge, B.; Meeussen, F.; Nies, E.; Berghmans, H.; Shen, D. Y. *Macromolecules* **2003**, *36*, 9145–9153.
- (15) Maeda, H. *Macromolecules* **1995**, *28*, 5156–5159.
- (16) Spevacek, J.; Hanykova, L.; Starovoytova, L. *Macromolecules* **2004**, *37*, 7710–7718.
- (17) Zeng, X. G.; Yang, X. Z. *J. Phys. Chem. B* **2004**, *108*, 17384–17392.
- (18) Nies, E.; Ramzi, A.; Berghmans, H.; Li, T.; Heenan, R. K.; King, S. M. *Macromolecules* **2005**, *38*, 915–924.
- (19) Ahad, E. *J. Appl. Polym. Sci.* **1987**, *22*, 1665–1676.
- (20) Kim, Y. S.; Dong, L.; Hickner, M. A.; Glass, T. E.; Webb, V.; McGrath, J. E. *Macromolecules* **2003**, *36*, 6281–6285.
- (21) Lorthioir, C.; Alegria, A.; Colmenero, J. *Phys. Rev. E* **2003**, *68*, 31805.
- (22) Havriliak, S.; Negami, S. *Polymer* **1967**, *8*, 161–210.
- (23) Cole, R. H.; Cole, K. S. *J. Chem. Phys.* **1942**, *10*, 98.
- (24) Davidson, D. W.; Cole, R. H. *J. Chem. Phys.* **1951**, *19*, 1484–1490.
- (25) Moran, G. R.; Jeffrey, K. R.; Thomas, J. M.; Stevens, J. R. *Carbohydr. Res.* **2000**, *328*, 573–584.
- (26) Hayashi, Y.; Shinyashiki, N.; Yagihara, S.; Yoshida, K.; Teramoto, A.; Nakamura, N.; Miyazaki, Y.; Sorai, M.; Wang, Q. *Biopolymers* **2002**, *63*, 21–31.
- (27) Cervený, S.; Schwartz, G. A.; Bergman, R.; Swenson, J. *Phys. Rev. Lett.* **2004**, *93*, 245702.
- (28) Starkweather, H. W. *Macromolecules* **1981**, *14*, 1277–1281.

- (29) Starkweather, H. W. *Polymer* **1991**, *32*, 2443–2448.
- (30) Ohmine, I.; Saito, S. *Acc. Chem. Res.* **1999**, *32*, 741–749.
- (31) Floriano, M. A.; Angell, C. A. *J. Chem. Phys.* **1989**, *91*, 2537–2543.
- (32) Barthel, J.; Bachhuber, K.; Buchner, R.; Hetzenauer, H. *Chem. Phys. Lett.* **1990**, *165*, 369–373.

MA050811T